JOURNAL OF THERMOPHYSICS AND HEAT TRANSFER
Vol. 7, No. 1, Jan.–March 1993

Flight Measurements of Low-Velocity Bow Shock Ultraviolet Radiation

Peter W. Erdman* and Edward C. Zipf†
University of Pittsburgh, Pittsburgh, Pennsylvania 15260
Patrick Espy‡ and Carl Howlett§
Utah State University, Logan, Utah 84322
Deborah A. Levin¶ and Richard Loda**
Institute for Defense Analyses, Alexandria, Virginia 22311
Robert J. Collins††
University of Minnesota, Minneapolis, Minnesota 55455
and
Graham V. Candler‡‡
North Carolina State University, Raleigh, North Carolina 27695

The ultraviolet spectrum, atomic oxygen 130.4-nm radiation intensity, total plasma density, and electron temperature of a Mach 12 bow shock were obtained by a sounding rocket experiment launched from the Wallops Flight Facility (WFF) on April 25, 1990 at 12:32 a.m. Eastern Standard Time (EST). A two-stage, Terrier Malamute rocket which attained an apogee of 720 km was used in this experiment. Optical data in the 200–400-nm wavelength range were obtained from 37 to 75 km at a vehicle velocity of 3.5 km/s at various locations on the 0.1016-m radius hemispherical dome. Electron probe and VUV OI 130.4-nm measurements were obtained near nose cone ejection at 37 km. This article presents a discussion of the instruments used and the key data obtained.

Introduction

THIS article deals primarily with the design of the bow shock ultraviolet (BSUV) payload and with the optical data obtained during the Terrier Malamute flight. The BSUV experiment was launched on April 25, 1990 at 12:32 a.m. Eastern Standard Time (EST) from NASA's Wallops Island Flight Facility (WFF). The complete payload weight was approximately 65 kg and the total flight time was 15 min. The up-leg portion of the trajectory is shown in Fig. 1. The rocket achieved the predicted apogee of 720 km. At second-stage motor burnout (37 km), the velocity was ~3.5 km/s as predicted by preflight trajectory simulations. During the observational phase of the flight the rocket performed as expected with the velocity remaining relatively constant from 37 to 75 km. Since heating of the spherical dome was predicted to be high during the ascent through the low atmosphere, it was protected by a cover that provided thermal protection and drag reduction. All instruments were operational at launch, with measurements beginning at the time of nose cone ejection (approximately 37-km altitude). Only ascent data will be presented here. A comparison between the experimental results and a state-of-the-art thermochemical, nonequilibrium flowfield code can be found in a companion article.[1]

Payload Instrument Description

The primary instrumentation on the payload included one rapid-scan spectrometer, eight quartz fiber optic photometers, one NO-filled CaF_2 window ionization chamber, and one electron density microprobe. Numerous temperature monitors provided support information. Figure 2 shows the arrangement of the instrumentation in the payload, whereas Fig. 3 shows a detail of the arrangement of the fiber optics as they looked through quartz windows in the dome. The microprobe and oxygen VUV sensor were mounted directly to the rocket nose. The photometer cluster is mounted at the rear, with fiber optics used to route signals around the spectrometer.

The rapid scanning spectrometer covered the 190–400-nm wavelength range in a 0.25-s scan. The instrument used a modified Fastie-Ebert design with a 150-mm focal length, 10

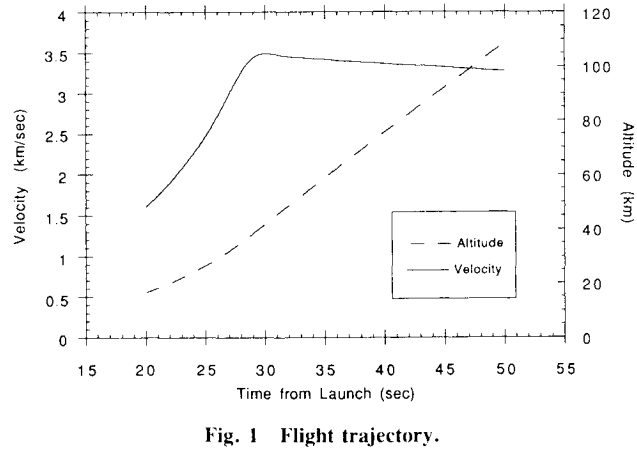

Fig. 1 Flight trajectory.

Presented as Paper 91-1410 at the AIAA 26th Thermophysics Conference, Honolulu, HI, June 24–26, 1991; received Dec. 4, 1991; revision received Feb. 27, 1992; accepted for publication Feb. 28, 1992.

*Research Associate, Department of Physics and Astronomy.
†Professor, Department of Physics and Astronomy. Member AIAA.
‡Research Associate Professor, Department of Physics.
§Technical Program Manager, Center for Space Engineering. Member AIAA.
¶Research Staff Member, Science and Technology Division. Member AIAA.
**Research Staff Member, Science and Technology Division.
††Professor, Department of Electrical Engineering.
‡‡Assistant Professor, Department of Mechanical and Aerospace Engineering.

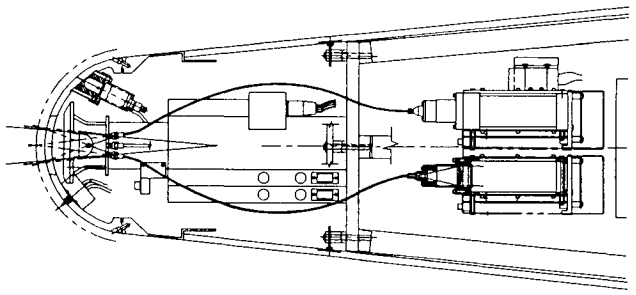

Fig. 2 Schematic of instrument layout in the rocket payload.

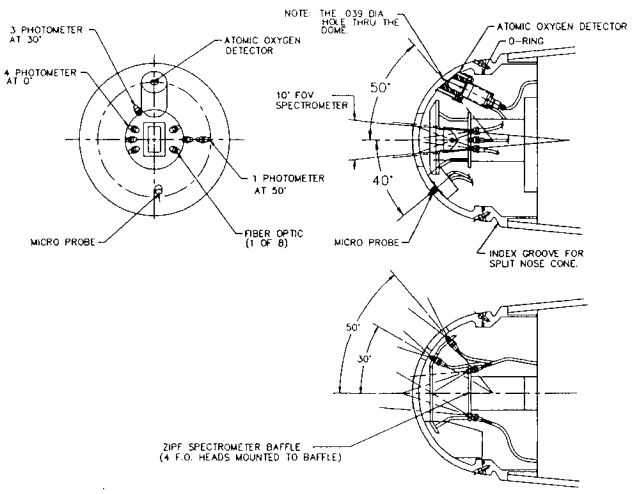

Fig. 3 Detail of the instruments' fields of view through the dome windows placed at indicated angles from the vehicle centerline.

deg (total angle) field of view (FOV), and two exit slits—each with its own photomultiplier detector. Equal width curved slits provided 1-nm resolution (at 400 nm) as a reasonable compromise between throughput and resolution. Optics were all Al-MgF_2 overcoated Zerodur, super-polished by Hyperfine, Inc., for reduced scattering. The grating was from a new 1800 g/mm classically ruled master also manufactured by Hyperfine, Inc. This was a very low-noise, highly efficient grating that considerably enhanced the effectiveness of this instrument. Each photomultiplier detector had completely separate high-voltage supplies and data systems, each with its own pulse-counting system which operated in parallel with an electrometer channel. The analog channel was designed to handle the very high signal levels anticipated near nose cone deployment when counting rates would be well beyond those which could be accommodated by a pulse-counting system alone. An additional increase in the dynamic range was accomplished with a photomultiplier gain increase of 10^2 several seconds after nose cone deployment. The analog signals were digitized with fast 16-bit A/D converters before transmission by the telemetry system. The high-speed stepper motor wavelength drive system made a 0.2-nm wavelength step every 384 μs in synchronization with the data system. This short integration time demanded very high instrument throughput in order to yield statistically significant counts per channel which become shot-noise limited even at very high counting rates.

Design considerations required 1) that the spectrometer have a high intrinsic dynamic range (10 orders of magnitude from maximum tolerable signal to signal/dark count noise ratio of unity); 2) that it acquire individual spectra rapidly; and 3) that it have very low scattered light levels. With the requirement of 0.25-s/scan to allow for approximately 1 km of altitude resolution, only ~35 scans could be accumulated in the ~9 s the rocket was between 37–75 km in altitude. The design requirements were dictated by the model predictions that the signal levels would drop approximately six decades in 6 s, hence, good altitude resolution and total dynamic range was very important for a successful measurement. The preflight signal predictions at altitudes of 50 km and higher, however, were too low by orders of magnitude.[1] The unintentional overdesign of the instrumentation provided an additional bonus in that data was obtained during a longer portion of the flight than anticipated.

The spectrometer's first goal was to measure bow shock ultraviolet radiance—primarily from the nitric oxide gamma-band system. The spectral range between the short wavelength cutoff of quartz at 190 and 400 nm was covered by two separate detectors with different photocathodes, one CsTe and the other Bialkali. The Bialkali detector was blocked to radiation beyond 420 nm and short of 240 nm by a Schott black glass filter. This reduced any concern about a longer wavelength source of scattered light as well as eliminated any second-order contamination from strong short wavelength radiation. One detector nominally covered the first hundred nanometers of the scan and the second detector covered the remainder. However, these detectors and their exit slit spacings were chosen to provide ~50-nm overlap in wavelength coverage for redundancy in case of the failure of one detector, and as a check on the independent calibrations of each channel and its data system. Excellent agreement between the two detectors was found in the reduced data, confirming that each performed nominally.

The filtered photometers were located on a lower deck in the payload and were coupled to the forward windows with quartz fiber optics. At the exit of this fiber, a lens focused on the small diameter fiber formed a parallel beam incident on an interference filter and then onto the photomultiplier. The photocathodes were selected according to the spectral feature of interest. These photometers were designed in two banks of four detectors, each with its own high-voltage supply. The individual detectors also had both an analog electrometer channel and a digital pulse counting channel in order to increase the total dynamic range to approximately eight orders of magnitude. The analog channels were digitized with a 16-bit A/D converter before transmission over the telemetry system with a sample rate of 548 samples/s.

Design considerations required that the photometers achieve the highest altitude resolution possible within the constraints of instrument size, sensitivity, and data rate. Along with the measurement of the bow shock ultraviolet radiance as a function of altitude and velocity, the variations in intensity with position from the stagnation point was also measured by this system of separate photometers with viewing angles of 0, 30, and 50 deg from the vehicle centerline. The total angle of the entrance FOV of each photometer was ~25 deg. Each photometer, its feature, and position is shown in Table 1. The redundancy in the first two photometers was to insure six orders of magnitude total measurement dynamic range and avoid detector saturation at the time of nose cone ejection. The detector recovery time characteristics were such that if driven into saturation at signal levels greater than anticipated at 40-km altitude, subsequent measurements at higher altitudes would have been lost.

Auxiliary measurements were obtained with an atomic oxygen sensor and a Langmuir microprobe. The atomic oxygen OI 130.4-nm sensor provided a measure of the atomic oxygen vacuum ultra violet (VUV) flux existing in the bow shock under optically thick conditions and of the atomic oxygen abundance in the shock-heated air. No dome window was used for this measurement, instead the diode was sealed directly to the inside of the dome and viewed through a small through-hole (1.0-mm diam). The detector was a NO-filled CaF_2 window ionization chamber. A simple Langmuir microprobe was also used to measure the electron density and temperature in the bow shock. Both of these instruments performed well and yielded data near the point of nose cone ejection.

Absolute calibrations for the spectrometer and the photometers were performed with a deuterium lamp. Cross cal-

Table 1 Photometer characteristics

$\lambda_0 \pm \Delta\lambda$, nm	Molecular feature	Position, deg	Minimum signal,[a] W/cm^{2}sr
1) 230.0 ± 30.0[b]	NO γ system	0	2.8×10^{-11}
2) 230.0 ± 30.0[c]	NO γ system	0	3.8×10^{-11}
3) 215.0 ± 3.0	NO γ (1, 0)	0	1.2×10^{-11}
4) 230.0 ± 30.0	NO γ system	30	1.4×10^{-10}
5) 230.0 ± 30.0	NO γ system	30	8.7×10^{-11}
6) 230.0 ± 30.0	NO γ system	50	1.8×10^{-12}
7) 309.0 ± 4.0	OH A-X (0, 0)	0	8.7×10^{-9}
8) 391.2 ± 2.5	N_2^+ 1NG (0, 0)	0	3.5×10^{-11}

[a]In-band. [b]High gain. [c]Low gain.

ibrations were also performed in the field under identical conditions in order to minimize the systematic errors. Separate transmission calibrations of the quartz viewing windows in the dome were performed on the actual flight windows. Dome temperatures of about 300 K were obtained from thermocouple measurements. Preflight calculation of UV attenuation through the window material (Corning 7940) showed that signal losses would be on the order of a few percent or less at the shortest wavelengths. No vacuum system was employed, hence the spectrometer data acquired below 200 nm will not be presented here. Several spectral line sources were used to properly locate the spectrometer wavelength scan and establish the wavelength interval. Excellent agreement has been found between the spectrometer and photometer flight measurements. The VUV gas diode was compared against an NBS-calibrated VUV diode to yield an absolute calibration for the oxygen 130.4-nm measurement. The microprobe was calibrated in a laboratory plasma system where the electron density and temperature could be measured with other independent techniques and cross-compared with the microprobe.

The entire payload was hermetically sealed and remained pressurized during the flight. Before launch, the payload was vigorously purged and then positively pressurized with dry Argon. This gas then continued to flow out the small viewing port used for the oxygen VUV measurement, thereby reducing the absorption of that radiation.

The rather high speed of 3.5 km/s achieved by the vehicle system was made possible by reducing the total payload weight to 65 kg. This was accomplished primarily through the extensive use of composite structural materials. The skin and nose cone were fabricated from aluminum honeycomb with graphite cloth facings, and the decks used aluminum-faced honeycomb. These efforts reduced the payload weight from that of an initial design by approximately 50% without any loss of structural strength.

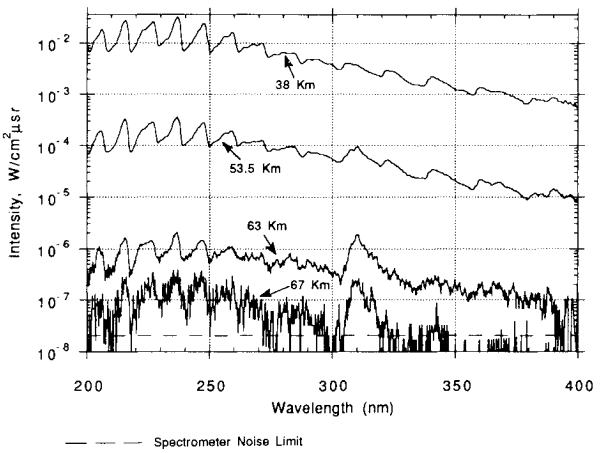

Fig. 4 Spectral scans of the ultraviolet bow shock radiation taken after the protective nose cone was deployed (~38 km) and at later flight times.

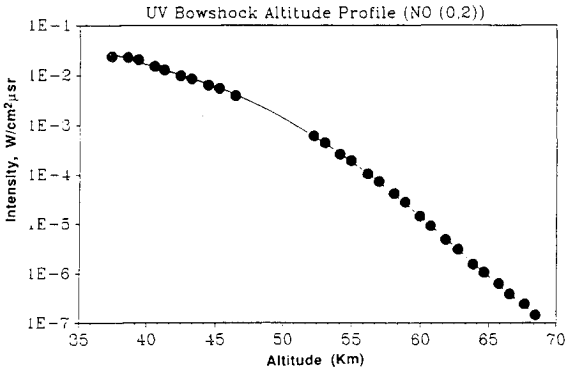

Fig. 5 Signal vs altitude for the NO(0, 2) gamma band, derived from spectrometer data.

Data

Postflight analyses showed that the spectrometer performed according to specifications throughout the flight. Figure 4 illustrates spectra merged from the short and long wavelength detectors, beginning at approximately 38 km in altitude. The signal from the NO photometer (no. 1) was used to correct the spectra for the intensity change with altitude. This effect involved a 20% correction during the course of a scan. The brightest features in the bow shock spectrum are probably all bands of nitric oxide created in the high-temperature shock wave. At 63 km the total signal levels differ by over four orders of magnitude from the scan at 38 km, but the spectral features are rather similar, except at the longer wavelengths where the OH (A → X) transition becomes evident.

A plot of intensity vs altitude for a single nitric oxide emission band [the (0, 2) gamma band] was taken from such spectrometer data and is shown in Fig. 5. The rate of fall off with altitude is much slower than predicted by the most recent multitemperature theoretical calculations (three orders of magnitude at 60 km), although the absolute intensity at the lowest altitude is in reasonable agreement with those calculations.[1]

All eight photometers also functioned well during the flight. The altitude profile for the NO wide-band photometer that concentrated on the extended NO gamma band (no. 1) is presented in Fig. 6 to indicate the high quality of the data available. The data were averaged over 0.25-s bins, and the dark-count rates and the average analog offsets determined just before launch have been removed. An integration of the spectrometer data from the 38-km scan (shown in Fig. 4) over the bandpass of the photometer's interference filter gives agreement on the order of 5% with the intensities measured by this photometer. Since the optical calibrations are nearly independent of one another, this increases our confidence in the absolute magnitude of the data.

Using simple molecular langmuir probe theory an electron temperature of 3850 K and a density of 2.5×10^{11} cm^{-3} give the best fit to the data obtained from the first full scan of the

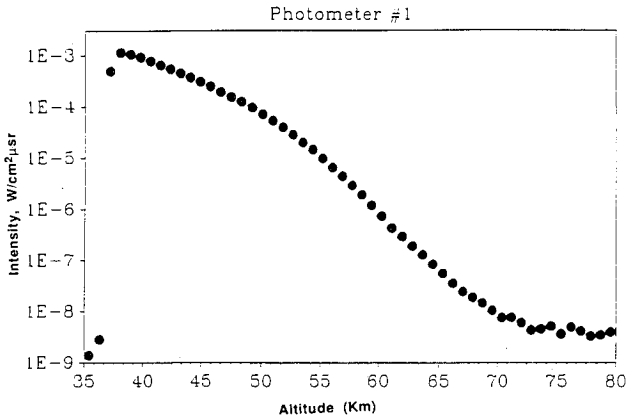

Fig. 6 Signal vs altitude from photometer no. 1, with bandpass of 60 nm, centered at 230 nm.

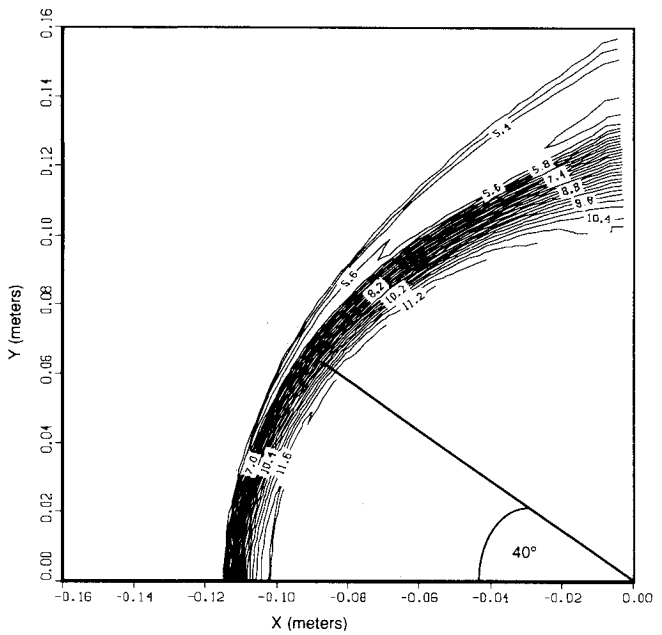

Fig. 7a Electron concentration contour levels, $\log_{10}$ (number/cm^3), at 40 km, 3.5 km/s, and nose radius of 0.1016 m.

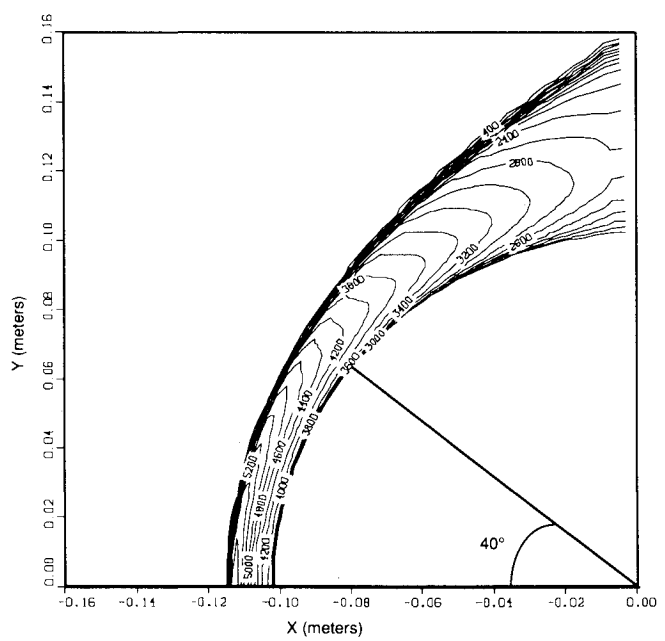

Fig. 7b Electron temperature contour levels K, for same flow conditions given for electron concentration contour plot.

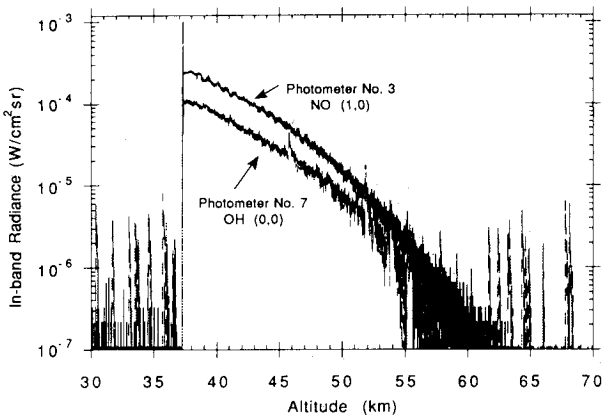

Fig. 8 In-band radiance as a function of altitude for the hydroxyl radical photometer (no. 7) compared with the narrow band NO photometer (no. 3).

microprobe after the nose cone was deployed. Initial fluctuations in the photometer data in the first few milliseconds after the nose cone deployment had dampened by this time, indicating that either the flow that was disturbed by nose cone ejection or initial transients in the detectors had reached stabilized levels. These values are, in fact, averages of the actual physical values over the 5-mm length of the microprobe, and so their interpretation may not be simple. Flowfield calculations of the electron temperature and density at an altitude of 40 km and a speed of 3.5 km/s given in Figs. 7a and 7b show good agreement with experimentally derived results at the probe location of 40-deg off-axis. The combination of heating and the corrosive action of the high atomic oxygen density in the shock region destroyed the probe wire after a few more scans, so no additional data were obtained.

Resonance radiation from atomic oxygen at 130.4 nm was measured by the nitric oxide photodiode. A value of 0.18 μW/cm^2/sr $\pm$ 50% was obtained shortly after the protective nose cone was deployed. The total dynamic range of this device was limited by uncertainties in the amplifier baseline drift, but the pronounced jump in signal at nose cone deployment allowed a reasonable measurement at that time. The measured value may serve as a source to elucidate differences in Monte Carlo entrapment vs classical radiative transport models.

The hydroxyl (OH) photometer (number seven) and the N_2^+ 1NG (0, 0) photometer (number eight) used phototubes that were not solar blind. Due to the low work-functions of these photocathodes, they exhibited a great deal of dark count noise. In Fig. 8 the in-band radiance from No. 7 is shown as a function of altitude. For comparison, the in-band radiance observed in the narrow band NO photometer (no. 3) is also shown. Even in the presence of the shot noise, the hydroxyl signal was seen to decay more slowly with altitude than that from nitric oxide photometer. The difference in altitude dependence can be explained in terms of the chemical kinetics in the shock layer.[1]

Conclusions

The flight experiment obtained for the first time optical data in the low-velocity, low-altitude flight regime. The ultraviolet shock-heated air spectrum was obtained from 200–400 nm between altitudes of 40–70 km. Photometer measurements at selected band passes provided accurate time correlation with spectrometer data and additional spatial information at 30 and 50 deg off-axis. Auxiliary data were obtained from electron probe, atomic oxygen, and thermocouple measurements.

The data have provided an opportunity to test for the first time the computational fluid dynamics and radiation models that were originally developed for a high-speed flight regime. The predictive capability is good at 40 km but by 50 km serious discrepancies between the experiment and modeling are evident; reasons for these discrepancies are discussed in Ref. 1.

Acknowledgments

The bow shock ultraviolet experiment (BSUV) was supported by the Innovative Science and Technology Office of the Strategic Defense Initiative Organization with the primary purpose of verifying aerodynamic and radiative transfer models applicable to boost phase conditions. The design, construction, and calibration of the payload instrumentation involved a collaborative effort among researchers at many institutions. Utah State University served as overall program manager, built the photometers and atomic oxygen resonance radiation detectors, and provided advanced materials payload research and construction. The University of Pittsburgh developed and fabricated a rapid scanning spectrometer and an electron probe. The Space Data Corporation was responsible for the telemetry, payload and vehicle integration, and provided launch support along with NASA's Wallops launch crew. The Institute for Defense Analyses was responsible for the optical radiation level predictions and interpretation of theory, whereas NASA/Ames provided assistance with the flowfield and radiation modeling as well as computer support. Fundamental aspects of the models have also been investigated by other groups under a related program managed by the Army Research Office.

Reference

[1]Levin, D. A., Candler, G. V., Collins, R. J., Erdman, P. W., Zipf, E., Espy, P., and Howlett, C., "Comparison of Theory with Experiment for the Bow Shock Ultraviolet Rocket Flight," *Journal of Thermophysics and Heat Transfer* (submitted for publication).